

Haijun Hou\*, H.J. Zhu, W.H. Cheng and L.H. Xie

# Elastic and Thermal Properties of Silicon Compounds from First-Principles Calculations

DOI 10.1515/zna-2015-0367

Received August 18, 2015; accepted May 24, 2016; previously published online June 16, 2016

**Abstract:** The structural and elastic properties of V-Si ( $V_3Si$ ,  $VSi_2$ ,  $V_5Si_3$ , and  $V_6Si_5$ ) compounds are studied by using first-principles method. The calculated equilibrium lattice parameters and formation enthalpy are in good agreement with the available experimental data and other theoretical results. The calculated results indicate that the V-Si compounds are mechanically stable. Elastic properties including bulk modulus, shear modulus, Young's modulus, and Poisson's ratio are also obtained. The elastic anisotropies of V-Si compounds are investigated via the three-dimensional (3D) figures of directional dependences of reciprocals of Young's modulus. Finally, based on the quasi-harmonic Debye model, the internal energy, Helmholtz free energy, entropy, heat capacity, thermal expansion coefficient, Grüneisen parameter, and Debye temperature of V-Si compounds have been calculated.

**Keywords:** Elastic; Thermal Properties; Vanadium-Silicides.

## 1 Introduction

Due to the potential chemical and physical properties, transition metal silicides draw much interest in high-temperature applications [1]. According to the V-Si binary phase diagram, there are four binary silicide compounds ( $A15-V_3Si$ ,  $C40-VSi_2$ ,  $D8m-V_5Si_3$ , and  $V_6Si_5$  with an orthorhombic structure) [2]. The V-Si compounds have

been studied for many years. For  $V_5Si_3$ , there are three phases with  $W_5Si_3$ -prototype,  $Mn_5Si_3$ -prototype, and  $Cr_5B_3$ -prototype, where the  $W_5Si_3$ -prototype phase is a stable structure [3]. We just study the  $W_5Si_3$ -prototype  $V_5Si_3$ . In order to obtain the structural and mechanical properties of the V-Si compounds, a number of works have been reported. Carcia and Barsch measured the pressure derivatives of the single-crystal elastic constants of  $V_3Si$  at 77 and 298 K [4]. Zhang et al. investigated the thermodynamic stability of  $V_6Si_5$  [5]. Zhang et al. also optimised thermodynamic modeling of the V-Si compounds by experiments [6]. The structural and electronic properties (electronic band structures and density of states) of  $V_3Si$ ,  $VSi_2$ ,  $V_5Si_3$ , and  $V_6Si_5$  have been investigated by using density functional calculations [7].

However, other studies have also studied the elastic constants of V-Si compounds using ultrasonic measurements [8]. In theoretical studies, elastic constants and the directional dependences of Young's modulus have not been discussed adequately but are important. In this work, we performed first-principles calculations for the elastic properties of  $V_3Si$ ,  $VSi_2$ ,  $V_5Si_3$ , and  $V_6Si_5$  consisting of elastic constants, bulk modulus, Young's modulus, shear modulus, Poisson's ratio, and directional dependences of Young's modulus. Based on the quasi-harmonic Debye model, Debye temperature, Grüneisen parameter, heat capacity, and thermal expansion coefficient of  $V_3Si$ ,  $VSi_2$ ,  $V_5Si_3$ , and  $V_6Si_5$  compounds are also investigated.

## 2 Method

The first-principles calculations are performed by using the plane wave method, as implemented in the CASTEP code [9], which has been shown to obtain the reliable results for the structural properties of various solids [10]. For structural property calculations, the exchange correlation potential is described in the generalised gradient approximation (GGA) using the Perdew–Burke–Ernzerhof (PBE) functional [11]. Vanderbilt-type ultrasoft pseudopotentials (USPPs) [12] are employed to describe the electron–ion interactions. Two parameters that affect the accuracy of calculations are the kinetic energy cutoff that determines the number of plane waves in the expansion and the number of special  $k$  points used for the Brillouin zone (BZ) integration. We performed convergence with respect to BZ

\*Corresponding author: Haijun Hou, School of Materials Engineering, Yancheng Institute of Technology, Yancheng 224051, China, E-mail: wyezhjhj@126.com

H.J. Zhu: School of Materials Engineering, Yancheng Institute of Technology, Yancheng 224051, China

W.H. Cheng: Department of Light Chemical Engineering, Yancheng Institute of Industry Technology, Yancheng 224005, China

L.H. Xie: Institute of Solid State Physics and School of Physics and Electronic Engineering, Sichuan Normal University, Chengdu 610068, China

sampling and the size of the basis set. Converged results are achieved with special  $k$ -points mesh  $10 \times 10 \times 10$  for  $V_3Si$ ,  $8 \times 8 \times 8$  for  $VSi_2$ ,  $5 \times 5 \times 4$  for  $V_5Si_3$ , and  $V_6Si_5$ , respectively. The size of the basis set is given by cutoff energy equal to 500 eV.

## 3 Results and Discussion

### 3.1 Structural Properties

In this article, the initial crystal structures are based on the experimental crystallographic data of V-Si compounds, and the lattice parameters of these compounds are optimised by using first-principle calculations. The crystal structures of V-Si compounds are shown in Figure 1. The optimised lattice parameters are listed in

Table 1, where the available experimental data and other theoretical results are included. For  $V_3Si$ , the calculated lattice parameters by the GGA-PBE method are in good agreement with the previous results (4.7001 Å) and other theoretical results [13, 15, 16]. For  $VSi_2$ , the calculated lattice parameters are found to be  $a = b = 4.5597$  Å,  $c = 6.3602$  Å, respectively, showing that they are in good agreement with the experimental values [17]. For  $V_5Si_3$ , the calculated lattice parameters are found to be  $a = b = 9.3997$  Å,  $c = 4.7252$  Å, respectively, are in good agreement with previous results [3, 7, 16]. For  $V_6Si_5$ , the calculated lattice parameters in this work are well consistent with the previous results [16, 18]. These agreements with the previous results provide a confirmation that this work is reliable.

The formation enthalpy  $E_f$  per atom of the  $V_xSi_y$  compounds can be expressed as

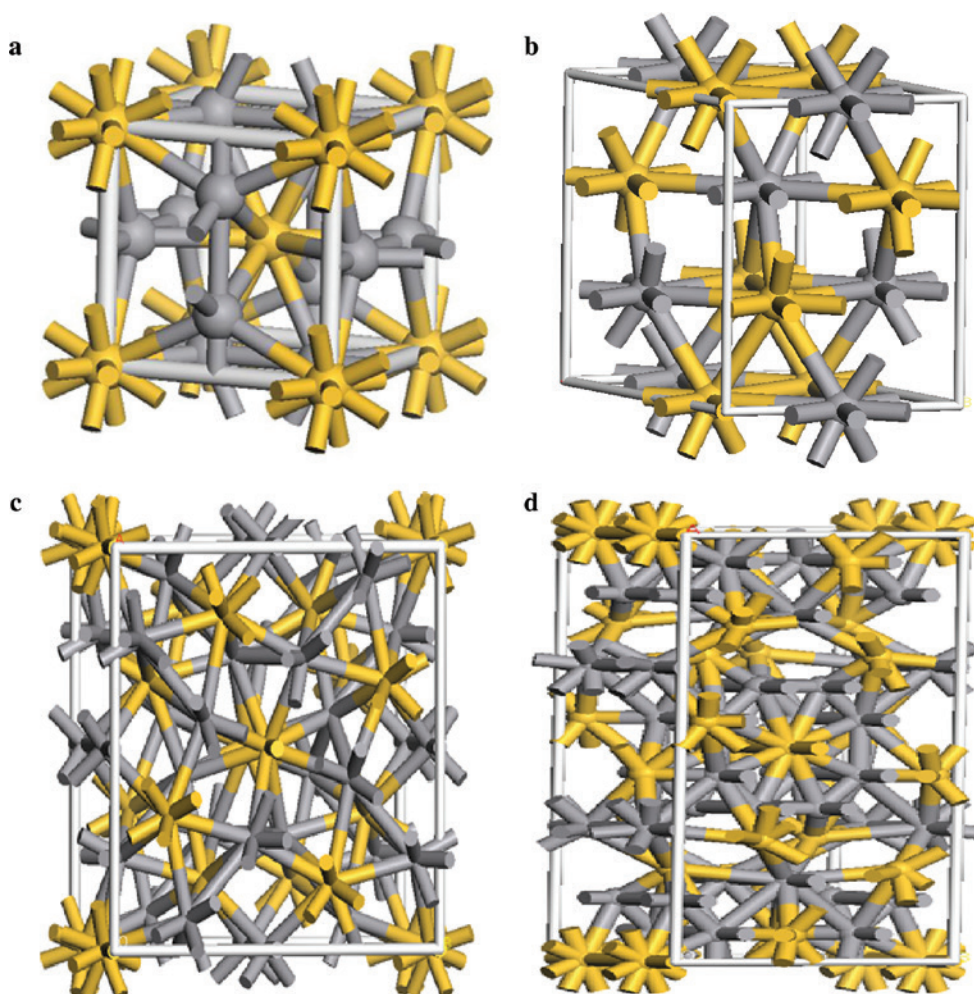


**Figure 1:** The crystal structure of V-Si compounds (a)  $V_3Si$ , (b)  $VSi_2$ , (c)  $V_5Si_3$ , and (d)  $V_6Si_5$  (The V atoms are shown as gray spheres and the Si atoms as yellow spheres.).

**Table 1:** Calculated results with other theoretical and experimental lattice parameters (Å) and formation enthalpy (kJ/mol) of the  $V_3Si$ ,  $VSi_2$ ,  $V_5Si_3$ , and  $V_6Si_5$ .

System	Space group	<i>a</i>	<i>b</i>	<i>c</i>	<i>E<sub>f</sub></i>
$V_3Si$	$pm3n$	4.7021 <sup>a</sup>			−44.78 <sup>a</sup>
		4.735 [13]			−38.75 [14]
		4.727 [15]			−46.4 [13]
		4.7001 [16]			−44.6 [16]
$VSi_2$	$p6_422$	4.5597 <sup>a</sup>	4.5597 <sup>a</sup>	6.3602 <sup>a</sup>	−54.26 <sup>a</sup>
		4.57 [17]	4.57 [17]	6.37 [17]	−45.91 [5]
$V_5Si_3$	$I4/mcm$	9.3997 <sup>a</sup>		4.7252 <sup>a</sup>	−59.55 <sup>a</sup>
		9.3930 [16]		4.7292 [16]	−56.5 [16]
		9.46 [7]		4.77 [7]	−53.73 [5]
		9.44 [7]		4.76 [7]	−59.00 ± 2 [13]
$V_6Si_5$	$Ibam$	9.3947 [3]		4.7265 [3]	−56.4 [3]
		15.9126 <sup>a</sup>	7.4859 <sup>a</sup>	4.8296 <sup>a</sup>	−54.27 <sup>a</sup>
		15.9419 [16]	7.4951 [16]	4.8100 [16]	−53 [16]
		15.966 [18]	7.501 [18]	4.858 [18]	−50.7 ± 2 [19–21]

<sup>a</sup>This work.

$$E_f = \frac{E_{tot}(V_xSi_y)}{x+y} - \frac{x E_{tot}(V) - y E_{tot}(Si)}{x+y} \tag{1}$$

where  $x$  and  $y$  are indices that give the amount of atoms of each atomic species within the unit cell of a structure  $V_xSi_y$ .  $E_{tot}$  is the total energy of atom of the elements or compound. The calculated formation enthalpies of  $V_3Si$ ,  $VSi_2$ ,  $V_5Si_3$ , and  $V_6Si_5$  are also listed in Table 1, together with available experimental data and other theoretical results. For  $V_3Si$ , the formation enthalpy  $E_f$  is in good agreement with previous results [13, 14, 16]. The formation enthalpy of  $VSi_2$  is also predicted in this work and in good agreement with theoretical results [5]. Compared to the experimental data [13], the present calculated formation enthalpy of the  $V_5Si_3$  is also in good agreement and is coherent with other theoretical results [3, 5, 16]. For  $V_6Si_5$ , the calculated formation enthalpy  $E_f$  (−54.27 kJ/mol) in this work is in good agreement with the value −53 kJ/mol obtained by the GGA-PBE method [16] and other previous measurement results [19–21]. The deviation is only 6.57%.

3.2 Elastic Constants

The number of independent elastic constants is different for various crystal structures. For a cubic crystal, it has three independent elastic constants ( $C_{11}$ ,  $C_{12}$ , and  $C_{44}$ ). For a hexagonal crystal, it has five independent elastic constants ( $C_{11}$ ,  $C_{12}$ ,  $C_{13}$ ,  $C_{33}$ , and  $C_{44}$ ). For a tetragonal chalcopyrite crystal, it has six independent elastic constants ( $C_{11}$ ,  $C_{12}$ ,  $C_{13}$ ,  $C_{33}$ ,  $C_{44}$ , and  $C_{66}$ ). For an orthorhombic crystal, it has nine elastic constants ( $C_{11}$ ,  $C_{22}$ ,  $C_{33}$ ,  $C_{44}$ ,  $C_{55}$ ,  $C_{66}$ ,  $C_{12}$ ,  $C_{13}$ , and  $C_{23}$ ). The mechanical stability criteria are given by [22–25].

As shown in Table 2, all of the elastic constants for  $V_3Si$ ,  $VSi_2$ ,  $V_5Si_3$ , and  $V_6Si_5$  compounds satisfy the respective mechanical stability criteria. It indicates that all above structures are mechanically stable. The elastic constants for  $V_3Si$  are in agreement with the experimental data (at  $T = 77$  K) [4]. It is worth pointing out that our theoretical calculations of the elastic constants for  $VSi_2$  with space group  $P6_422$  are in agreement with the experimental data [17]. The  $C_{ij}$  values

**Table 2:** Calculated results with other theoretical and experimental elastic constants  $C_{ij}$  (GPa) of the compounds in  $V_3Si$ ,  $VSi_2$ ,  $V_5Si_3$ , and  $V_6Si_5$ .

System		$C_{11}$	$C_{12}$	$C_{13}$	$C_{22}$	$C_{23}$	$C_{33}$	$C_{44}$	$C_{55}$	$C_{66}$
$V_3Si$	This work	241.78	169.56					78.60		
	[4]	233.6	151					77.1		
$VSi_2$	This work	375.46	62.70	76.39			426.99	144.94		
	[17]	357.8	50.6	68.1			422.3	135.7		
$V_5Si_3$	This work	397.23	104.46	99.91			341.07	104.09		129.06
	[3]	401.7	106.7	99.6			351.1	103.1		127.8
$V_6Si_5$	This work	392.70	123.69	80.59	331.60	91.74	343.01	136.12	98.89	114.54

**Table 3:** Calculated results with other theoretical and experimental bulk modulus  $B$  (GPa), shear modulus  $G$  (GPa), Young modulus  $E$  (GPa), Poisson's ratio  $\sigma$ , the ratio of the shear modulus  $G$  to the bulk modulus  $B$ , the compressional wave  $V_p$  (m/s), the shear velocities  $V_s$  (m/s), and average wave velocity  $V_m$  (m/s) of the compounds in  $V_3Si$ ,  $VSi_2$ ,  $V_5Si_3$ , and  $V_6Si_5$ .

System		$B$	$G$	$E$	$\sigma$	$B/G$	$V_p$	$V_s$	$V_m$
$V_3Si$	This work	193.64	57.52	157.01	0.364	3.37	6939.3	3154.8	3554.1
	[8]	213					7116	3819	
$VSi_2$	This work	178.29	153.15	357.18	0.166	1.16	9060.4	5733.2	6307
	Exp. [17]	167.2	147.9	342.6	0.158				
$V_5Si_3$	This work	193.26	121.69	301.74	0.239	1.59	8213.4	4805.3	5328.5
	[3]	195.8	122.1	303.1	0.24	1.60	8150	4755	5274
$V_6Si_5$	This work	183.71	120.16	295.95	0.232	1.53	9910.7	5858	6489.7
	[8]						7818	4380	

calculated by the GGA-PBE method of  $V_5Si_3$  are also provided and compared. The calculated  $C_{ij}$  values in this work are well consistent with the previous results [3]. Unfortunately, there are no other theoretical and experimental results for comparison with our elastic results for  $V_6Si_5$ .

It is known that the mechanical properties are determined by the elastic modulus. The polycrystalline elastic properties, including bulk modulus  $B$ , shear modulus  $G$ , Young modulus  $E$ , and Poisson's ratio  $\sigma$ , can be obtained by Voigt–Reuss–Hill (VRH) approximation. The  $B$ ,  $G$ , and  $E$  are listed in Table 3. As can be seen from Table 3, the bulk modulus  $B$  of for V-Si compounds follows the order  $V_3Si > V_5Si_3 > V_6Si_5 > VSi_2$ .  $V_3Si$  has the largest bulk modulus (193.64 GPa). The Young's modulus of for the  $V_3Si$ ,  $VSi_2$ ,  $V_5Si_3$ , and  $V_6Si_5$  compounds follows the order  $VSi_2 > V_5Si_3 > V_6Si_5 > V_3Si$ .

According to Pugh's criterion [26], the ductility or brittleness of a solid material is judged by  $B/G$  ratio. The critical value which separates ductile and brittle material is  $B/G = 1.75$ . If  $B/G > 1.75$ , behaves in a ductile manner. Otherwise, behaves in a brittle. Moreover, the Poisson's ratio  $\sigma$  is consistent with  $B/G$ , which refers to a ductile compound has a large  $\sigma > 0.26$  [27]. The values of  $B/G$  are larger than 1.75 and values of  $\sigma$  are larger than 0.26 for  $V_3Si$  in Table 3, which testify that they are ductile. The values of  $B/G$  and  $\sigma$  for  $VSi_2$ ,  $V_5Si_3$ , and  $V_6Si_5$  are less than 1.75 and 0.26, respectively. It shows that they are all brittle.

The values of the compressional velocity wave  $V_p$  and the shear wave velocity  $V_s$  can be obtained using the Navier's equation [28], where  $\rho$  is density of the compound.

$$V_p = \sqrt{\left(B + \frac{4}{3}G\right) \frac{1}{\rho}} \quad (2)$$

$$V_s = \sqrt{\frac{G}{\rho}} \quad (3)$$

The average wave velocity  $V_m$  can be calculated by

$$V_m = \left[ \frac{1}{3} \left( \frac{2}{V_s^3} + \frac{1}{V_p^3} \right) \right]^{-1/3} \quad (4)$$

The calculated sound velocity of  $V_p$ ,  $V_s$ , and  $V_m$  for the  $V_3Si$ ,  $VSi_2$ ,  $V_5Si_3$ , and  $V_6Si_5$  compounds are listed in Table 3. In comparison, the calculated values of  $V_p$  and  $V_s$  for  $V_3Si$  at zero pressure are a little lower than reported by Fleischer et al. [8]. For  $VSi_2$ , the calculated values of  $V_p$  and  $V_s$  are in good agreement with those reported by Fleischer et al. [8]. For  $V_5Si_3$ , the calculated  $V_p$  and  $V_s$  in this work are in agreement with the values by the VASP-GGA method [3] and other previous results [8]. Without experimental data and theoretical results of the  $V_6Si_5$ , we cannot make any comparisons. We expect that our theoretical results provide the valuable reference for the further research.

As a method to study the elastic anisotropic behavior of a solid material, the 3D surface constructions of the directional dependences of reciprocals of Young's modulus  $E$  are very useful. The expressions of the reciprocals of Young's modulus for the  $V_3Si$ ,  $VSi_2$ ,  $V_5Si_3$ , and  $V_6Si_5$  compounds are different for each other due to their various crystal structures [22].

In Figure 2, we show the mechanical stable structures of  $V_3Si$ ,  $VSi_2$ ,  $V_5Si_3$ , and  $V_6Si_5$  compounds. The surface in each graph represents the magnitude of Young's modulus  $E$  along different orientations. From this figure, we can clearly see that the Young's modulus shows some anisotropy at different orientations. It also should be noted that the Young's modulus of  $V_3Si$  shows slight anisotropy and the Young's modulus of  $VSi_2$ ,  $V_5Si_3$ , and  $V_6Si_5$  shows some anisotropy for different orientations. As for the hexagonal  $VSi_2$ , the 3D directional dependences of the Young's modulus along  $z$  axis are more compressible than along  $x$ - and  $y$ -axes. The 3D figure of the Young's modulus for



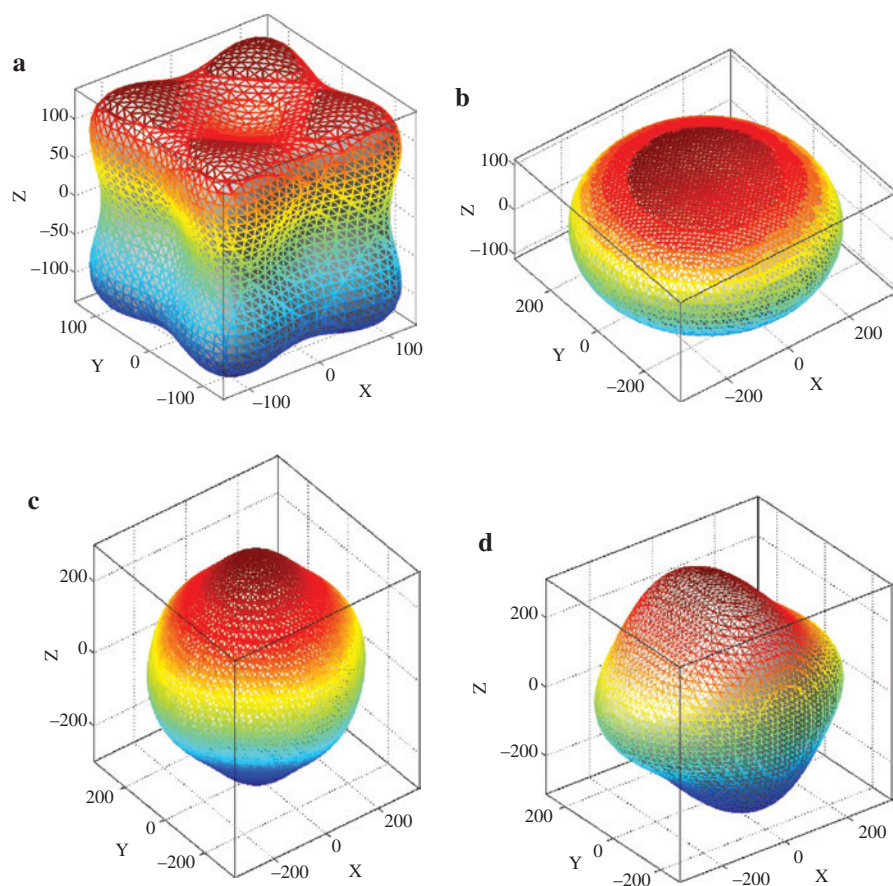


**Figure 2:** The directional dependence of the Young's modulus for the  $V_3Si$ ,  $VSi_2$ ,  $V_5Si_3$ , and  $V_6Si_5$  compounds [(a)  $V_3Si$ , (b)  $VSi_2$ , (c)  $V_5Si_3$ , and (d)  $V_6Si_5$ ]. The magnitude of Young's modulus at different directions is represented by the contour. The units are in GPa.

the tetragonal  $V_5Si_3$  is characterised by more anisotropic along the  $z$ -axis than that along the  $x$ - and  $y$ -axes. As for the orthorhombic  $V_6Si_5$ , the 3D surface of Young's modulus along  $x$ -,  $y$ -, and  $z$ -axes is shown highly anisotropic.

### 3.3 Thermal Properties of $V_3Si$ , $VSi_2$ , $V_5Si_3$ , and $V_6Si_5$ under High Temperature and High Pressure

In order to investigate the thermal properties of  $V_3Si$ ,  $VSi_2$ ,  $V_5Si_3$ , and  $V_6Si_5$  compounds under high pressure (0–25 GPa) and melting points temperature [6], we have used the quasi-harmonic Debye model as implemented in the Gibbs code [29]. First, we obtain a set of total energy results versus unit-cell volumes around the equilibrium geometry. Then, the above-mentioned results are fitted to the equation of state in order to obtain different parameters as a function of pressure and temperature from standard thermal relations. By the above-mentioned method, we can get the internal energy  $U$ , the

heat capacity of constant volume  $C_v$ , the heat capacity at constant pressure  $C_p$ , the entropy  $S$ , the thermal expansion coefficient  $\alpha$ , Debye temperature  $\Theta$ , and Grüneisen parameter  $\gamma$ .

The thermal properties of the  $V_3Si$ ,  $VSi_2$ ,  $V_5Si_3$ , and  $V_6Si_5$  compounds are calculated at the different temperatures ranging from 0 to about melting points. The pressure effect is investigated in the range 0–25 GPa. Heat capacity belongs to one of the most important thermal properties of the materials. Figure 3 shows the calculated heat capacity at constant volume as functions of the temperature under zero GPa. It can be seen from Figure 3 that the heat capacity  $C_v$  increases exponentially with the temperature at  $T < 400$  K. At higher temperature,  $C_v$  follows the Debye model and approaches the Dulong–Petit limit indicating the thermal energy at high temperature excites all phonon modes.

As an important physical quantity, the Debye temperature could distinguish the physical properties between high- and low-temperature regions. The variation of the Debye temperature  $\Theta$  (K) as a function of pressure and

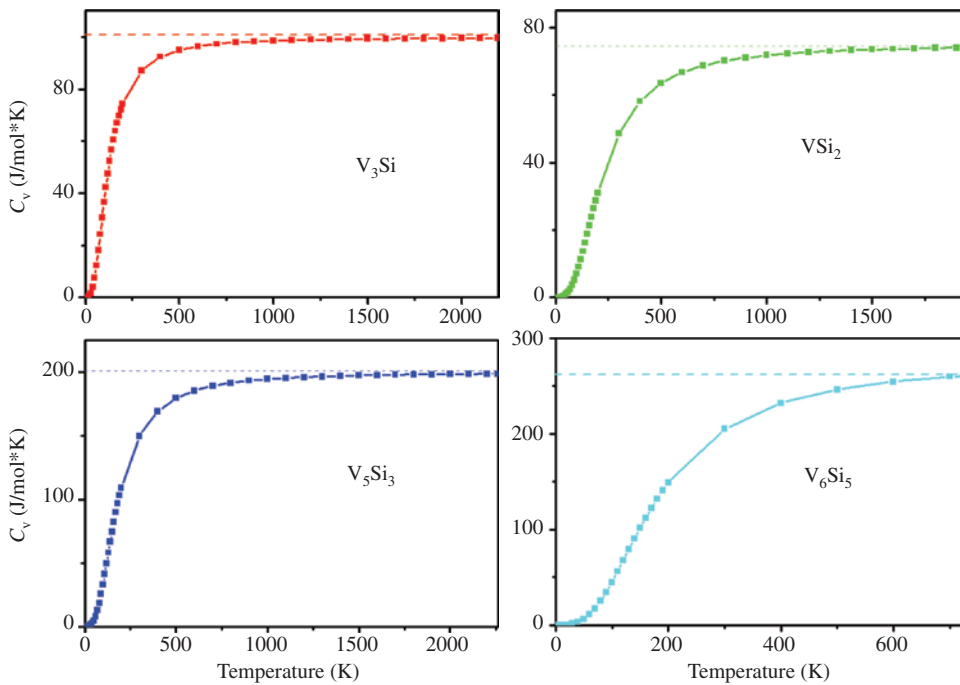


Figure 3: The heat capacity of constant volume  $C_v$  (J/mol K) for  $V_3Si$ ,  $VSi_2$ ,  $V_5Si_3$ , and  $V_6Si_5$  in V-Si compounds at 0 GPa.

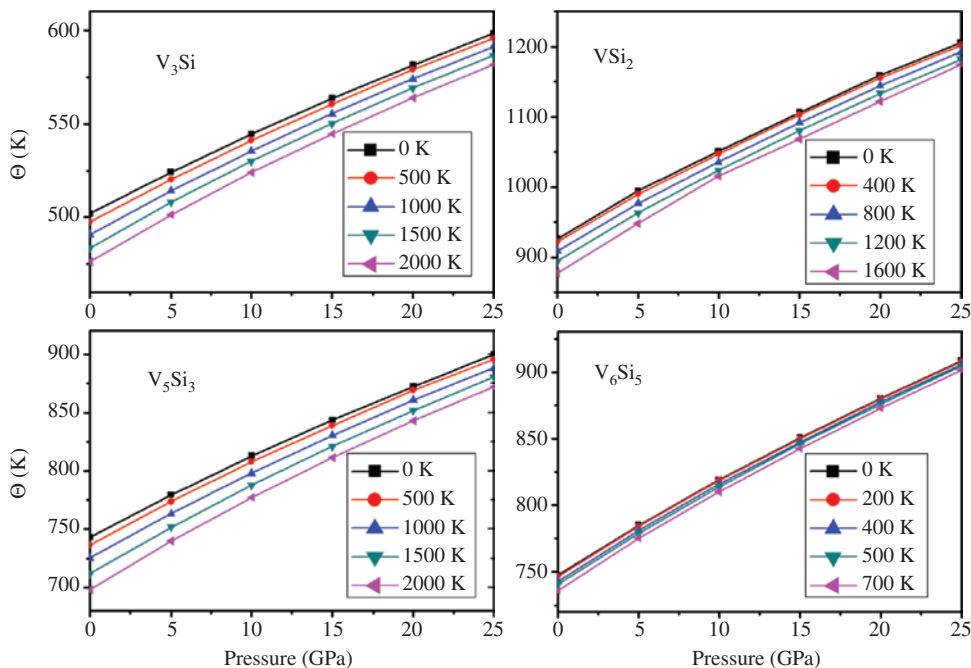


Figure 4: Debye temperature versus pressure at various temperatures for  $V_3Si$ ,  $VSi_2$ ,  $V_5Si_3$ , and  $V_6Si_5$ .

temperature is displayed in Figure 4. With the applied pressure increasing, the Debye temperatures are almost linearly increasing. The temperature and pressure dependence of  $\Theta$  (K) reveals that the thermal vibration frequency of atoms in V-Si ( $V_3Si$ ,  $VSi_2$ ,  $V_5Si_3$ , and  $V_6Si_5$ ) compounds changes with temperature and pressure.

Figure 5 shows the volume thermal expansion coefficient  $\alpha$  of  $V_3Si$ ,  $VSi_2$ ,  $V_5Si_3$ , and  $V_6Si_5$  across different pressures, from which it can be seen that the volume thermal expansion coefficient  $\alpha$  increases quickly at a given temperature particularly at zero pressure below the temperature of 300 K. After a sharp increase, the volume thermal

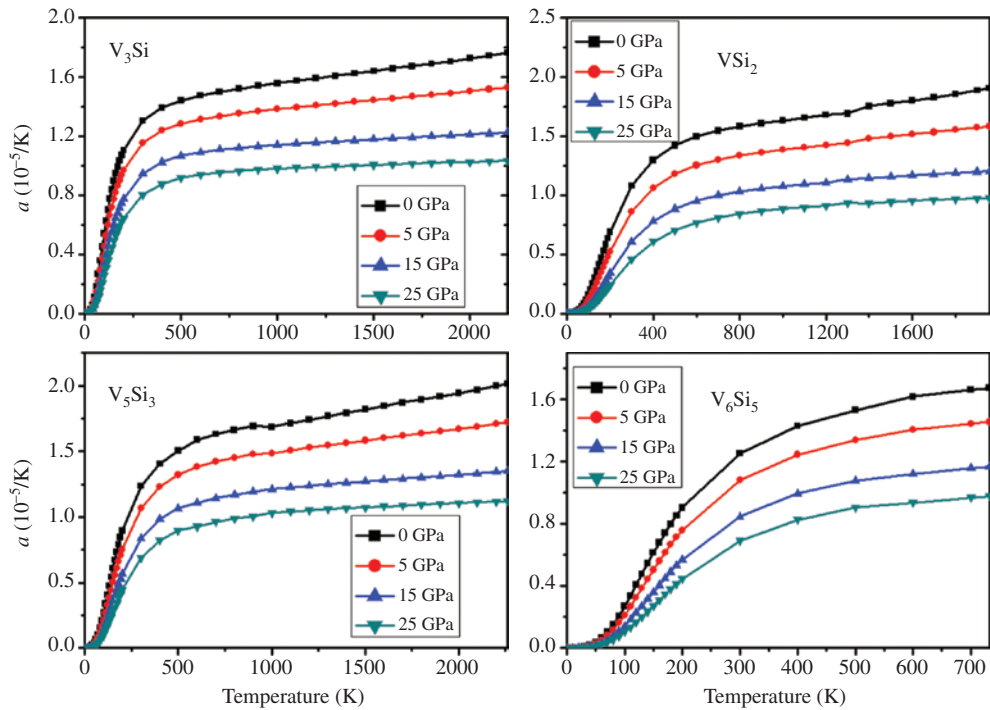


Figure 5: Thermal expansion coefficients versus temperature at various pressures for  $V_3Si$ ,  $VSi_2$ ,  $V_5Si_3$ , and  $V_6Si_5$ .

Table 4: The calculated internal energy  $U$  (kJ/mol), heat capacity of constant volume  $C_v$  (J/mol\*K), heat capacity of constant pressure  $C_p$  (J/mol\*K), Helmholtz free energy  $A$  (kJ/mol), entropy  $S$  (J/mol\*K), Debye temperature  $\Theta$  (K), Grüneisen parameter  $\gamma$ , and thermal expansion coefficient  $\alpha$  ( $10^{-5}/K$ ) for  $V_3Si$ ,  $VSi_2$ ,  $V_5Si_3$ , and  $V_6Si_5$  at 300 K under different pressures.

$P/GPa$	$U$	$C_v$	$C_p$	$A$	$S$	$\Theta$	$\gamma$	$\alpha$
$V_3Si$								
0.00	33.96	87.19	87.79	7.35	88.69	499.87	1.768	1.31
5.00	34.31	86.15	86.66	8.85	84.87	522.37	1.705	1.16
10.00	34.65	85.17	85.61	10.19	81.56	543.00	1.653	1.04
15.00	34.98	84.24	84.62	11.40	78.62	562.16	1.609	0.95
20.00	35.30	83.35	83.69	12.40	75.98	580.12	1.571	0.87
25.00	35.60	82.50	82.80	13.52	73.59	597.14	1.537	0.80
$VSi_2$								
0.00	32.07	48.60	49.01	22.82	30.83	923.96	2.593	1.08
5.00	33.38	45.81	46.10	25.14	27.48	991.74	2.463	0.86
10.00	34.54	43.49	43.71	27.05	24.97	1049.19	2.369	0.72
15.00	35.69	41.31	41.48	28.84	22.80	1104.18	2.289	0.61
20.00	36.82	39.25	39.39	30.55	20.91	1157.32	2.221	0.52
25.00	37.84	37.51	37.62	32.02	19.40	1203.72	2.166	0.46
$V_5Si_3$								
0.00	76.91	149.88	150.97	42.94	113.23	740.44	1.973	1.24
5.00	78.52	145.85	145.85	46.70	106.07	777.18	1.899	1.07
10.00	80.06	142.12	142.12	50.08	99.93	811.02	1.837	0.94
15.00	81.51	138.69	139.25	53.11	94.67	841.96	1.786	0.84
20.00	82.90	135.46	136.00	55.90	90.01	871.07	1.742	0.76
25.00	84.25	132.42	132.98	58.49	85.86	899.48	1.704	0.69
$V_6Si_5$								
0.00	106.01	205.42	206.93	59.67	154.47	744.86	1.952	1.25
5.00	108.31	199.72	200.94	64.97	144.45	782.62	1.877	1.08
10.00	110.48	194.45	195.46	69.71	135.90	817.31	1.815	0.95
15.00	112.53	189.62	190.47	73.95	128.60	848.99	1.764	0.85
20.00	114.51	185.08	185.81	77.87	122.13	878.78	1.719	0.76
25.00	116.44	180.75	181.39	81.54	116.32	907.18	1.680	0.69

expansion coefficient of the  $V_3Si$ ,  $VSi_2$ ,  $V_5Si_3$ , and  $V_6Si_5$  is nearly insensitive to the temperature above 300 K due to the electronic contributions. Thermal expansion coefficient  $\alpha$  strongly decreases with pressure at a constant temperature.

Finally, we have also calculated the internal energy  $U$ , entropy  $S$ , thermal expansion coefficient  $\alpha$ , heat capacity  $C_V$  and  $C_P$ , Helmholtz free energy  $A$ , Grüneisen parameter  $\gamma$ , and Debye temperature  $\Theta$  for the  $V_3Si$ ,  $VSi_2$ ,  $V_5Si_3$ , and  $V_6Si_5$  in V-Si at 300 K under different pressures. The theoretical results are presented in Table 4. However, there has been no experimental and theoretical data available for the thermal properties of  $V_3Si$ ,  $VSi_2$ ,  $V_5Si_3$ , and  $V_6Si_5$  compounds so far. Therefore, our calculated results can provide support for future works on  $V_3Si$ ,  $VSi_2$ ,  $V_5Si_3$ , and  $V_6Si_5$  compounds.

## 4 Conclusions

We have investigated the structural, elastic properties, elastic anisotropy, and thermodynamic properties of  $V_3Si$ ,  $VSi_2$ ,  $V_5Si_3$ , and  $V_6Si_5$  compounds using first-principles calculations. The calculated elastic constants of compounds indicate that the  $V_3Si$ ,  $VSi_2$ ,  $V_5Si_3$ , and  $V_6Si_5$  compounds are mechanically stable. Bulk modulus, shear modulus, Young's modulus, and Poisson's ratio have also been calculated and discussed. Moreover, we found that the pressure and temperature have important effects on the internal energy, heat capacity, Helmholtz free energy, entropy, Debye temperature, Grüneisen parameter, and thermal expansion coefficient.

**Acknowledgments:** This project was supported by the Natural Science Foundation of China (Grant nos. 51402251 and 51502259). This work was sponsored by the Natural Science Foundation of Jiangsu Province of China (BK20130428). This work was supported by the joint research fund between Collaborative Innovation Center for Ecological Building Materials and Environmental Protection Equipments and Key Laboratory for Advanced Technology in Environmental Protection of Jiangsu Province (GX2015305), and Natural Science Foundation of the Higher Education Institutions of Jiangsu Province (Grant no. 14KJD430003). This work was supported by the science and technology project from Ministry of Housing and Urban-Rural Development of the People's Republic of China (2015-K4-007). This work was supported by

Top-notch Academic Programs Project of Jiangsu Higher Education Institutions, TAPP (Grant no. PPZY2015A025).

## References

- [1] B. P. Bewlay, M. R. Jackson, J. C. Zhao, P. R. Subramanian, M. G. Mendiratta, et al., *MRS Bull.* **28**, 646 (2003).
- [2] T. B. Massalski, J. L. Murray, L. H. Bennett, and H. Baker (Eds.), *Binary Alloy Phase Diagrams*, ASM Metals Park, OH 1990.
- [3] X. M. Tao, H. M. Chen, X. F. Tong, Y. F. Ouyang, P. Jund, et al., *Comput. Mater. Sci.* **53**, 169 (2012).
- [4] P. F. Carcia and G. H. Barsch, *Phys. Stat. Sol. (b)* **59**, 595 (1973).
- [5] C. Zhang, J. Wang, Y. Du, and W. Q. Zhang, *J. Mater. Sci.* **42**, 7046 (2007).
- [6] C. Zhang, Y. Du, W. Xiong, H. H. Xu, P. Nash, et al., *Calphad* **32**, 320 (2008).
- [7] M. B. Thieme and S. Gemming, *Acta. Metall.* **57**, 50 (2009).
- [8] R. L. Fleischer, R. S. Gilmore, and R. J. Zabala, *Acta. Metall.* **37**, 2801 (1989).
- [9] V. Milman, B. Winkler, J. A. White, C. J. Packard, M. C. Payne, et al., *Int. J. Quantum Chem.* **77**, 895 (2000).
- [10] H. J. Hou, F. J. Kong, J. W. Yang, L. H. Xie, and S. X. Yang, *Phys. Scr.* **89**, 065703 (2014).
- [11] J. P. Perdew, K. Burke, and M. Ernzerhof, *Phys. Rev. Lett.* **77**, 3865 (1996).
- [12] D. Vanderbilt, *Phys. Rev. B* **41**, 7892 (1990).
- [13] S. V. Meschel and O. J. Kleppa, *J. Alloys Compd.* **267**, 128 (1998).
- [14] E. K. Storms and C. E. Myers, *High Temp. Sci.* **20**, 87 (1985).
- [15] Y. F. Lomnytska, *Powder Metall. Met. Ceram.* **46**, 461 (2007).
- [16] C. Colinet and J. C. Tedenac, *Comput. Mater. Sci.* **85**, 94 (2014).
- [17] F. Chu, M. Lei, S. A. Maloy, J. J. Petrovic, and T.E. Mitchell, *Acta Mater.* **44**, 3035 (1996).
- [18] P. Spinat, R. Fruchart, and P. Herpin, *Bull. Soc. Fr. Mineral. Cristallogr.* **93**, 23 (1970).
- [19] V. N. Eremenko, G. M. Lukashenko, and V. R. Sidorko, *Rev. Intl. Hautes Temp. Refract.* **12**, 237 (1975).
- [20] V. N. Eremenko, G. M. Lukashenko, V. R. Sidorko, and O. G. Kulik, *Dopov. Akad. Nauk Ukr. RSR Ser. A* **38**, 365 (1976).
- [21] V. N. Eremenko, G. M. Lukashenko, and V. R. Sidorko, *Dopov. Akad. Nauk Ukr. RSR Ser. B* **36**, 712 (1974).
- [22] J. F. Nye, *Physical Properties of Crystals*, Oxford University Press, Oxford 1985.
- [23] Q. K. Hu, Q. H. Wu, Y. M. Ma, L. J. Zhang, Z. Y. Liu, et al., *Phys. Rev. B* **73**, 214116 (2006).
- [24] M. Born and K. Huang, *Dynamical Theory of Crystal Lattices*, Clarendon Press, Oxford 1954.
- [25] O. Beckstein, J. E. Klepeis, G. L. W. Hart, and O. Pankratov, *Phys. Rev. B* **63**, 134112 (2001).
- [26] S. F. Pugh, *Philos. Mag.* **45**, 823 (1954).
- [27] J. J. Lewandowski, W. H. Wang, and A. L. Greer, *Philos. Mag. Lett.* **85**, 77 (2005).
- [28] K. B. Panda and K.S. Ravi Chandran, *Comput. Mater. Sci.* **35**, 134 (2006).
- [29] M. A. Blanco, E. Francisco, and V. Luaa, *Comput. Phys. Commun.* **158**, 57 (2004).